Melt dynamics of supramolecular comb polymers: Viscoelastic and dielectric response

Mariapaola Staropoli, Andreas Raba, Claas H. Hövelmann, Marie-Sousai Appavou, Jürgen Allgaier, Margarita Krutyeva, Wim Pyckhout-Hintzen, Andreas Wischnewski, and Dieter Richter

Citation: Journal of Rheology **61**, 1185 (2017);

View online: https://doi.org/10.1122/1.5001059

View Table of Contents: http://sor.scitation.org/toc/jor/61/6

Published by the The Society of Rheology

Melt dynamics of supramolecular comb polymers: Viscoelastic and dielectric response

Mariapaola Staropoli,[a] Andreas Raba, and Claas H. Hövelmann

JCNS-1 and ICS-1, Forschungszentrum Jülich GmbH, Leo-Brandt-Straße, 52425 Jülich, Germany

Marie-Sousai Appavou

Jülich Centre for Neutron Science (JCNS) at MLZ, 85747 Garching, Germany

Jürgen Allgaier, Margarita Krutyeva, Wim Pyckhout-Hintzen, Andreas Wischnewski, and Dieter Richter

JCNS-1 and ICS-1, Forschungszentrum Jülich GmbH, Leo-Brandt-Straße, 52425 Jülich, Germany

(Received 3 May 2017; final revision received 8 August 2017; published 1 November 2017)

Abstract

The structure and the dynamics of supramolecular comblike polymers in the melt state is studied by a combination of linear rheology, dielectric spectroscopy, and small angle neutron scattering. The system consists of blends of 1,2-polybutyleneoxide (PBO) entangled backbones, randomly functionalized with thymine (thy) and barely entangled PBO graft chains—modified with 2,4-diamino-1,3,5-triazine (DAT) end groups. These bioinspired groups associate into a transiently branched comb architecture through heterocomplementary interaction involving the two different hydrogen bonding groups thy and DAT. In the present manuscript, we focus on the comparison of the macroscopic dynamics of the associating blends and permanent comb analogs. The viscoelastic and dielectric response of covalent and reversible combs are found to be comparable. The viscoelastic response of mixtures of thy-functionalized entangled backbones and DAT-end-modified barely entangled chains show a relaxation mechanism, which is mostly attributed to the association/breakage dynamics of the transient bonds with characteristic time ~ 1 s at $T = -25\,^{\circ}$C. In the parallel dielectric investigation, the reversible branched structure is still evident from the comparison with the corresponding permanent combs and allows the distinction between fixed arms relaxation and the lifetime. A α^* process of the thy-thy association is likewise detected. The time scale of the supramolecular association makes the thy-DAT pair an ideal candidate for the development of responsive materials that combine permanent and transient linkages for novel applications and self-healing properties. © *2017 The Society of Rheology*. [http://dx.doi.org/10.1122/1.5001059]

I. INTRODUCTION

Supramolecular polymers have gained increasing interest in the last decades due to the wide variety of novel properties which can be imparted to polymeric materials [1–3]. The introduction of reversible interactions in a covalent polymer system leads to additional dynamic processes on the time scale of the supramolecular bond lifetime and to a wide field of properties depending on the strength and density of the transient bonds. Most commonly used supramolecular interactions are metal-ligand complexes [4], ionic forces [5], $\pi - \pi$ interactions [6], and hydrogen bonds [7,8]. Of these, hydrogen bonding represents the most prominently used interaction due to the high directionality and reversibility and to the broad range of bond strengths, which can vary by several orders of magnitudes depending on the nature and functionality of the bonding groups. Supramolecular polymers can be divided in two main categories: End-functionalized linear chains [9–12] and side-functionalized backbones carrying several functional groups. The simplest example of hydrogen bonding associating polymers consisting of linear end-functionalized units gives rise to long supramolecular chains. In this simple case, the assembly of the functionalized units is well described by the theory of polycondensation of classical monomers. Besides linear association mechanisms, several examples of side-functionalized building blocks have been reported in the literature [13]. Side-chain functionalization offers an important tool to control the architecture and the properties of the resulting supramolecular polymer. The presence of several associating groups connected to a polymer chain and the aggregation of functional groups competing with the specific hydrogen bonding can lead to more complex supramolecular architectures than linear, and therefore, to more complex dynamics [14–16]. Here, they are distinguished between self and heterocomplementary associations, depending on the interaction between two identical groups or two different groups, respectively. The influence of the transient bonds on the dynamics and the macroscopic mechanical properties of supramolecular polymers was investigated in several works [17,18]. The time scale of the association/dissociation as well as its temperature dependence in a supramolecular polymer have an important effect on the relaxation mechanism of a mechanical shear stress. The whole

[a]Author to whom correspondence should be addressed; electronic mail: m.staropoli@fz-juelich.de

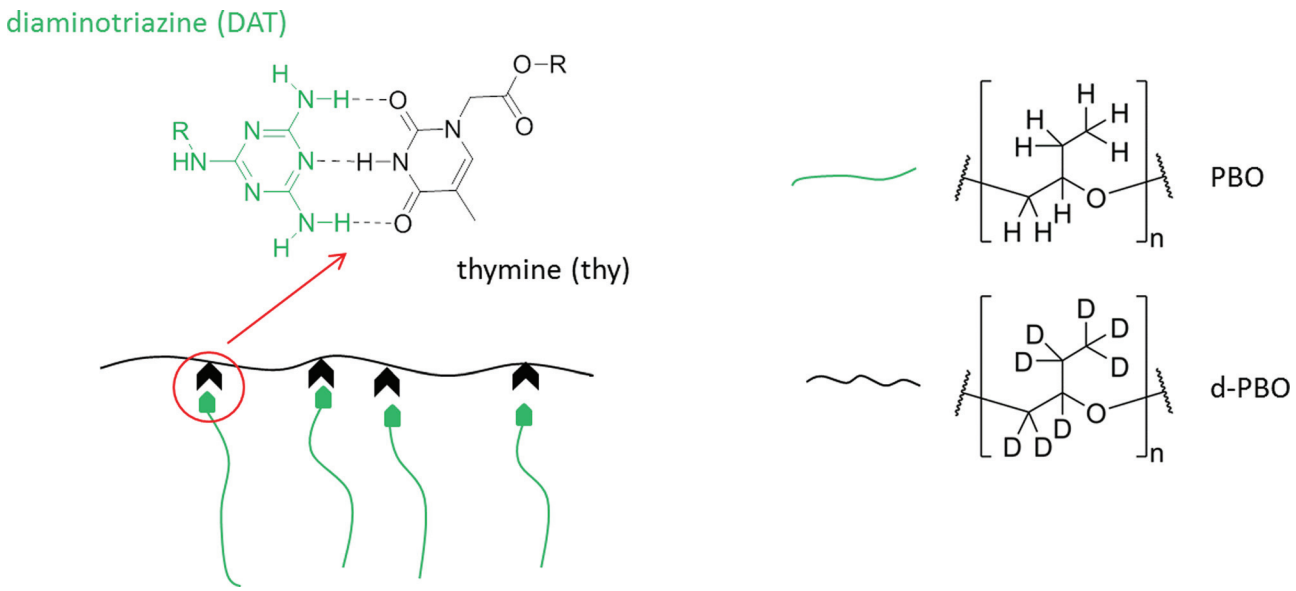

SCHEME 1. Schematic representation of the transient comb formed through thy-DAT hydrogen-bonding interactions.

dynamics may be totally dominated by the association/breakage of the transient bonds in case of unentangled functionalized chains, but it is far more complex in associating entangled polymers, where the relaxation behavior is determined by several further processes with different temperature dependence.

In this work, we study supramolecular comb structures based on hydrogen bonding between thymine (thy) and 2,4-diamino-1,3,5-triazine (DAT) functionalized 1,2-polybutyleneoxide (PBO) chains in the melt state. Recently, virtually exclusive heterocomplementary association could be observed in the supramolecular association of end-modified PEG bearing thy and DAT groups [10]. The structural investigation by small angle neutron scattering (SANS) was then extended to branched systems where randomly thy-functionalized PBO backbones and DAT end-functionalized shorter chains were found to interact via heterocomplementary association [19]. For this purpose an appropriate contrast between the backbone and graft arms was induced by means of H/D isotopic labeling as illustrated in Scheme 1.

Rheological measurements evidenced that this system can be described as a comb within the lifetime of the reversible bonds and as a simple blend of linear chains at longer times. In this work, we report further SANS results and present a comparison of the rheological and dielectric response of such reversible combs with the covalent analogs. Although the SANS investigation at room temperature revealed differences between the scattering of permanent and reversible combs, which have to do with the equilibrium and labeling of the system, we will show that the viscoelastic and dielectric behavior for the two systems are comparable. This result was related to the effective lifetime of the transient bonds, which leads to the observation of a comblike structure in a broad frequency range. In the direct comparison with the monofunctional compounds, the dielectric response confirmed roughly the time scale of linear rheology. This work, therefore presents a unique combination of techniques, applied to model covalent and supramolecular comb polymers and identifies both structure and characteristic time scales in a homogeneous melt state. Therefore, hydrogen-bonded combs result to be novel responsive materials that simultaneously exihibit the classical properties of comb polymer melts within the life time of the supramolecular formed H-bonds and those of a more easily processable blend at long times. The present experimental time scales can be ideally exploited in mechanical probing in the order of the Hz scale at ambient temperatures, which would allow autonomous self-healing or dampening to happen in combination with a permanently crosslinked network.

II. EXPERIMENTAL SECTION

A. Synthesis

All polymers were prepared by anionic ring-opening polymerization with subsequent chemical modification [20]. For alkylene oxides, exclusively head-to-tail (H-T) orientation occurs with no appearance of H−H or T-T junctions. We refer to the supplementary material document for the synthetic details and exact characterization [21]. Table I lists

TABLE I. Polymer codes and functionalization degree.

Backbones	thy groups per chain	Number of entanglements per chain (Z)
d-PBO 80k	0	10±0.4
d-PBO 80k-thy	∼15	
PBO 40k-thy	∼8	
Arms	DAT groups per chain	
PBO 15k	0	1.8±0.1
PBO 15k-DAT	1	
Permanent combs	Number of arms	
PBO 40k/PBO 15k Comb[a]	∼7	5±0.2
d-PBO 80k/PBO 15k Comb[a]	∼15	

[a]Permanent Combs are based on the backbones and arms specified before. The volume fraction of the backbone in the Permanent Combs is $\phi_b \sim 0.25$.

the polymer codes used in the manuscript and the degree of functionalization of the polymers studied. Proton NMR spectroscopy was used for the determination of the degree of functionalization [20]. All mixtures of different polymers were prepared by mixing stock solutions in pentane. The solvent was then removed under high vacuum for 4 days. For rheology and dielectric spectroscopy experiments, the polymer melts were used directly after removing the solvent.

B. Small angle neutron scattering

SANS experiments were performed using the KWS-2 diffractometer at MLZ (Garching, Germany) [22] using sample-to-detector distances between 20 and 1.35 m and $\lambda = 5$Å, covering a q-range between 3×10^{-3} Å^{-1} and 1×10^{-1} with $q = (4\pi/\lambda)\sin(\theta/2)$ where θ is the scattering angle. For the absolute scaling to cm^{-1}, the incoherent scattering level of Plexiglas® was used. The two-dimensional data were corrected for empty cell scattering, detector sensitivity, and background noise using B_4C as beam blocker and radially averaged. The incoherent background was determined from the high q-range and was in good agreement with the estimated incoherent scattering of the hydrogenous polymer fraction. Power law scattering, $I(q) \sim q^{-4}$ observed at low q was attributed to small voids present in the samples and the high contrast between these and the deuterated components. This contribution was subtracted entirely from the experimental data.

C. Rheology

Oscillatory shear experiments were carried out on a strain-controlled ARES (Rheometrics Sci Ltd.) rheometer using the parallel plate geometry. The diameter of the plates was 8 mm and the sample gap about 1 mm. Isothermal frequency sweeps were performed in a frequency range between $0.1 < \omega < 100$ rad/s. A temperature range between $-55 < T < -5$ °C with $\Delta T = 10$ °C under a nitrogen blanket within the linear rheology regime of the polymers was chosen. Master curves were obtained at a reference temperature T_{Ref} of −25 °C for each sample. For all samples analyzed the horizontal shift factor a_T for the construction of the master curves follows a WLF behavior to a very good approximation indicating a rather simple thermorheological behavior. T_g glass transition temperature values of all polymers were determined by DSC (Q2000, TA Instruments) with heating and cooling rates of 10 °C/min. The average T_g is (-66.4 ± 1.3) °C and variations ΔT_g are within ∼2 °C for all samples.

D. Dielectric spectroscopy

Dielectric relaxation measurements were performed on a Broadband Dielectric Converter (Novocontrol) in combination with an Alpha-A-High-Resolution-Analyzer (Novocontrol). The accessible frequency range for the dielectric function measurement is $10^{-3} - 10^{7}$Hz and the temperature control is operated by a Quatro Cryosystem. The sample was positioned between Au-plated electrodes of 20 mm diameter and with a constant gap of 0.05 mm controlled by spacers. The dielectric response for all the samples examined is reported at $T = -25$°C. No time-temperature shifting is necessary due to the inherent broad frequency range of ∼10 decades. To resolve the terminal mode of the shorter covalent comb more clearly, only measurements from a higher T were included.

III. THEORETICAL MODELS

As the manuscript is based on the synergy of several methods, each of which brings an important aspect of the supramolecular association, we briefly have to review the main computations and approaches toward this aim. We refer to the literature as well as to the text books for more detailed descriptions. Whereas the neutron scattering description and the linear rheology for branched polymers and their mixtures with linear material are well known, the description of the dielectric response for higher-generation branched architectural polymers is highly undeveloped and stops at the star polymer case [23]. Since the PBO monomer is asymmetric, it has both parallel and perpendicular dipole moment components to the chain contour. It is a typical A-type polymer like polyisoprene. Comblike structures have, to our best knowledge, hardly been studied yet [24] and differ considerably from star polymers through the pronounced hierarchical relaxation path of graft arms and backbones. Therefore, the discussion of the dielectric mode spectrum will be restricted to the identification of similarities between the different samples covering associating mixtures and covalent combs.

A. Scattering random phase approximation model

The scattering function of an isotopic diblock comb copolymer formed by a deuterated backbone and protonated arms (as shown in Scheme 1) is described by means of the random phase approximation (RPA) formalism. The RPA applies in general to binary blends of polymers with different scattering length density and its expression for a diblock copolymer in which the components are correlated is written in terms of the bare noninteracting structure factors [25,26] where we dropped the q-dependence for clarity only as follows:

$$\frac{d\Sigma}{d\Omega}\Big/\frac{\Delta\rho^2}{N_A} = S_{RPA} = \left(S_{ii}\cdot S_{aa} - S_{ia}{}^2\right)\Big/\left(\left(S_{ii} + S_{aa} + 2S_{ia}\right) - \frac{2\chi_{ia}}{\upsilon_0}\left(S_{ii}\cdot S_{aa} - S_{ia}{}^2\right)\right). \quad (1)$$

χ_{ia} is an effective Flory–Huggins parameter and takes into account the interaction between the H- and D-components. Since the Hildebrandt solubility parameters for PBO and the respective end-groups are virtually identical, no enthalpic effect of the H-bonding groups is expected to contribute to the miscibility. υ_0 is the monomeric volume of the PBO unit. $\Delta\rho^2$ is the contrast factor and N_A is Avogadro's constant. The contributions of the unperturbed form factors to the partial structure factors in Eq. (1), on the assumption of a Gaussian statistics, is reported in the literature [27,28] and given by

$$\begin{aligned} S_{aa} &= \phi_{ab} \cdot v_0 \cdot (N_a \cdot n_a) \cdot P_{aa}, \\ S_{ii} &= \phi_i \cdot v_0 \cdot (N_i \cdot n_i) \cdot P_{ii}, \\ S_{ia} &= \sqrt{\phi_{ab} \cdot \phi_i \cdot (N_i \cdot n_i) \cdot (N_a \cdot n_a) \cdot v_0^2 P_{aa} \cdot P_{ii}}, \end{aligned} \tag{2}$$

i and a stand, respectively, for the deuterated macromonomer blocks of the backbone (i) and for the protonated arms (a). N_i is the total number of blocks of length n_i in the backbone and N_a corresponds to the number of arms of length n_a attached.

The combination of the partial structure factors defined in Eq. (2) in the RPA expression gives rise to a correlation peak resulting from the alternation of *i(D)* and *a(H)* units within the same macromolecule. The scattering function of a comb structure, therefore shows a peak of which the amplitude and position is determined by the length of the correlation block *a…i…a*. The case of a random blend of linear homopolymers, which arises from the disconnection of the arms from the backbone, is recovered when the cross-term S_{ia} is set to zero and results in a Debye-like function [25] with a finite scattering at low q. For the particular case of a reversible comb, however, the equilibrium between a comblike structure and free components has to be considered in the definition of the RPA expression. The description of a multiblock copolymer/linear homopolymer mixture is accomplished by splitting the total fraction of short chains in two components $\phi_{ab,}$ ϕ_{af}, related to the volume fraction of arms correlated, i.e., bonded (b) and uncorrelated, i.e., free (f) with respect to the deuterated backbone. The maximum aggregation number, attainable in the equilibrium between thy and DAT is then determined by the backbone functionality and the contribution of the inherently present free arms leads to the finite scattering at low q. Thus, the application of the RPA formalism to our model system allows an accurate estimation of the *average* number of arms as well as the estimation of the equilibrium between the associating and free chains in the case of the reversible comb. SANS results for covalent and transient combs reported here, thus define the structure of the polymers investigated by both rheology and dielectric spectroscopy. For the full SANS characterization we refer to our previous work [19].

B. Rheology model description

As the equilibrium of transient combs depends on the temperature, the lifetime of the supramolecular bonds is also temperature dependent. If the latter are very long in reference to the time of observation, the dynamical response is that of a permanent comb. If on the other hand, the lifetime of associations is much shorter, the dynamics of a bimodal blend will be expected. As in the former SANS investigation [19] performed for $T > 5\,^{\circ}\mathrm{C}$, combs were clearly observed, we may conclude that the equilibrium constant is large enough at high T to allow the average arm functionality to be studied here. In this work, we therefore refer to the hierarchical model developed by Inkson *et al.* for the description of the linear rheology of permanent combs [29]. This model is based on the tube theory and predicts the hierarchical relaxation process typical of such a branched architecture. As a consequence of this hierarchical mechanism relaxing from-the-outside-inward, the fast retracted arms reduce the effective entanglement density of the main chain and accelerate the terminal relaxation time of the backbone reptation process. This is reflected in the relaxation modulus $G(t)$ of a comb polymer, which typically exhibits two rubbery plateaus: One at short times (higher frequency) attributed to entangled branches before their retraction, followed by a second one at longer times (lower frequency) related to the diluted backbone [30,31]. It is, therefore, different from that of a star branched polymer and resembles an H-polymer [32]. The reduction of the effective elastic modulus due to the dilution effect at a certain time t is correlated to the fraction of unrelaxed backbone segments ϕ_b by

$$G(\phi, t) = G_N^0 \phi_b^{\alpha+1}(t), \tag{3}$$

where G_N^0 is the plateau modulus at infinite short times and α is the dilution exponent. In this work, we assume $\alpha = 1$ for the description of melt conditions. Scheme 2 illustrates a comb composed of a backbone with n_b monomers and f grafted arms each containing n_a monomers. Although the functional groups are randomly distributed on the PBO backbone investigated, we assume a constant average distance between the connected branches as proposed by the present model. The number of entanglements Z for backbone and arms is defined using the molar mass of an entanglement strand, i.e., $Z = nm_0/M_e$ where m_0 and M_e are, respectively, the monomer mass and the entanglement molecular weight. The arm volume fraction ϕ_a is given as function of f and correlated to the backbone volume fraction ϕ_b by incompressibility as

$$\phi_a = fn_a/(fn_a + n_b) \quad \phi_b = 1 - \phi_a. \tag{4}$$

In the model, the relaxation of the arms occurs by retraction along the x_a coordinate, which runs from 0 at the free end to 1 at the branching point. The relative displacement that a segment performs is determined and controlled by the functional form of an entropic potential barrier $U(x_a, \phi_a, Z_a, \alpha)$ which is a function of the number of entanglements (Z_a) as well as the volume fraction of the arms. Since U is an implicit function but its exact formulation unimportant in this small review, we have omitted the exact expression and refer to the literature [29].

The retraction is an activated process and depends on the length of the chain. Within small fluctuations along the x_a coordinate, the branches perform a Rouse-like fluctuation along the primitive path and the early retraction time $\tau_{ae}(x_a)$ of the arms is independent on the potential. The transition to an activated relaxation time $\tau_{al}(x_a)$ occurs at a certain value of the coordinate x_a and the potential $U(x_a)$ then becomes effective. The cross-over function between the Rouse-like and the activated process defines the arm relaxation time scale $\tau_a(x_a)$ which is given by

$$\begin{aligned} \tau_a(x_a) &= \frac{\tau_{ae}(x_a) e^{U_a(x_a)}}{1 + \tau_{ae}(x_a) e^{U_a(x_a)} / \tau_{al}(x_a)} \\ &= \left(\frac{1}{\tau_{ae}(x_a)} e^{U_a(x_a)} + \frac{1}{\tau_{al}(x_a)} \right)^{-1}. \end{aligned} \tag{5}$$

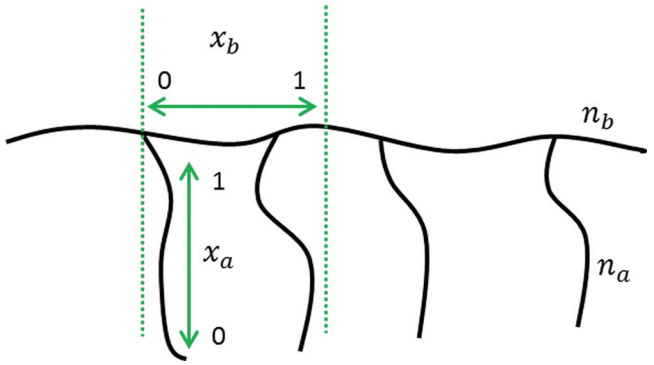

SCHEME 2. Representation of a comb polymer with $f = 4$.

For $\tau_a(1)$ the completely retracted branches act in diluting the backbone as in a θ solvent, and at the same time, in providing extra friction at the branching points. The terminal relaxation time is now attributed to the backbone reptation inside the dilated tube and is also affected by the diffusion of the branching points. The latter is taken into account by a parameter p^2. Here, we assume $p^2 = 1/12$ as in the reference work of Inkson. In the frame of the dynamic tube dilution, as in the constraint release process (CR), the backbone relaxation is dominated by the hops of the branching points when the arms have undergone a complete retraction along the coordinate x_a. In the reference model, the backbone coordinate ranges from 0 to 1 at the center of the chain. Similarly to the arms, an early relaxation process with time $\tau_{be}(x_b)$ occurs by fluctuation of the chain ends. The late relaxation time $\tau_{bl}(x_b)$ is correlated to the retraction of the inner segments of the backbone, collocated between the branching points. The transition between the fluctuation and the reptation mode, when the backbone is entangled, occurs at a certain value of the x coordinate (x_c) with an effective potential $U(x_b, x_c, \phi_b, Z_b, \alpha)$. For $x_b > x_c$ the reptation mode dominates the dynamics. The terminal relaxation time $\tau_{bb}(x_b)$ is associated to the terminal relaxation time of a comb, and therefore, attributed to the diluted backbone reptation and defined similarly as

$$\tau_{bb}(x_b) = \frac{\tau_{be}(x_b) e^{U_b(x_b)}}{1 + \tau_{be}(x_b) e^{U_b(x_b)} / \tau_{bl}(x_b)}. \tag{6}$$

The total relaxation modulus for the comb is expressed as a sum of two contributions taking into account, respectively, the arm retraction process and the backbone relaxation

$$G(t) = G_N^0(\alpha+1)\left(\int_0^1 {\phi_b}^{\alpha+1}(1-x_b)^{\alpha} e^{-(t/\tau_{bb}(x_b))} dx_b + \int_0^1 (1-\phi_a x_a)^{\alpha}\phi_a e^{-(t/\tau_a(x_a))} dx_a\right). \tag{7}$$

Theoretical predictions of the loss modulus G'' for the systems studied in the present work, PBO 40k/PBO 15k Comb and d-PBO 80k/PBO 15k Comb, respectively, are reported in Fig. 1 in order to analyze the sensitivity of the model to our experimental data. Moreover, the effect of the volume fractions of the components (ϕ_a and ϕ_b) on the hierarchical relaxation process is examined here.

Independent of the backbone length a broad maximum in G'' appearing at $\sim$1 rad/s is related to the retraction time of the 15k arms $\tau_a(x_a)$. For the 40k backbone comb, other than for the 80k case, the terminal relaxation mechanism associated to the diluted backbone cannot be identified anymore. The apparent lack of the hierarchical relaxation is related to the very comparable arm retraction $\tau_a(x_a)$ defined in Eq. (5) and the diluted backbone reptation time $\tau_{bb}(x_b)$ [Eq. (6)]. For the same reason, a very low sensitivity of G'' to f is observed and the low frequency range is only slightly affected by the average number of arms. For d-PBO 80k/PBO 15k Comb the more effective separation in frequency observed between the two characteristic times $\tau_a(x_a)$ and $\tau_{bb}(x_{bb})$ results in the distinction of two separate relaxation processes, and therefore, a stronger effect of the low frequency range. The calculation shows also that an increase of the number of arms, and therefore, of ϕ_a leads to a stronger dilution effect, as defined in Eq. (3), and to a less effective separation of τ_a and τ_{bb}. In the previous work [19], we noted that reversible combs based on PBO seemed to be characterized by a hierarchical relaxation mechanism similarly to a permanent one, but instead relaxation processes, which correspond, respectively, to the lifetime of the transient bonds, and the reptation of the backbone in a diluted tube are involved. The timely separation between the two mechanisms is strongly determined by the size of the arms and backbone. Therefore, depending on the temperature, the transiently branched system studied in this work could be described as a comblike structure within the lifetime of the bonds and as a simple blend at longer times. However, a general molecular model for the description of the reversible comb is missing and would involve consideration of CR events for bimodal blends as well, and therefore, we will refer to a qualitative comparison with the permanent structure. Depending on the characteristic times of the processes involved, the comblike behavior can dominate over

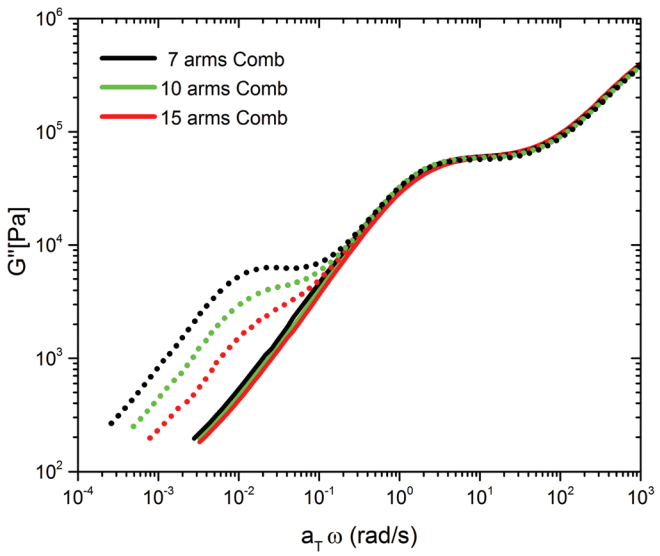

FIG. 1. Loss moduli calculated for PBO 40k/PBO 15k Comb (solid lines) and d-PBO 80k/PBO 15k Comb (dotted lines) at $T_{\mathrm{Ref}} = -25\,^{\circ}\mathrm{C}$.

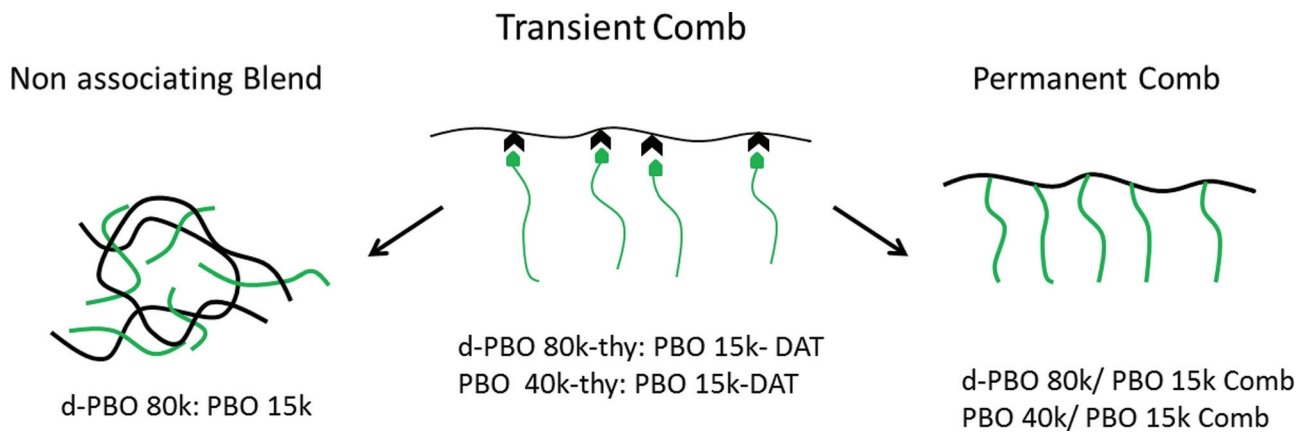

SCHEME 3. Schematic representation and nomenclature of the systems studied.

the simple blend or *vice versa*. If hydrogen bonds would open before or during the retraction strong effects into the direction of simple blends would have been expected. However, this effect will be of utmost interest for extensional viscosity measurements in which strain hardening should occur. On the other hand, the arms are barely entangled and no strong entropic penalty for retraction inside the tube may be expected.

IV. EXPERIMENTAL RESULTS

In this section, the results obtained for reversible combs resulting from the combination of thy- and DAT-functionalized PBO will be presented in parallel with analogs permanent combs. Nonassociating mixtures with identical composition, analyzed in previous publications, will be discussed only in the dielectric section. Scheme 3 illustrates the reversible comb in comparison with the reference systems: Permanent combs and nonassociating blends, respectively. The composition of the functionalized and nonassociating mixtures is summarized in Table II. The molar ratio is referred to the hydrogen bonding groups in the functionalized mixtures and is kept constant in the nonassociating blends in order to maintain the identical composition for all the samples analyzed.

A. Small angle neutron scattering

SANS results for functionalized mixtures of H (a) and D (i)-components and the permanent comb are presented in Fig. 2. The comparison between the permanent and reversible combs clearly evidences the effect of the equilibrium between associating and free arms on the scattering function. The q-dependence at high scattering vectors displays a power law with slope -2, characteristic for unperturbed Gaussian chains in both cases. In the scattering profile of the functionalized mixture (red) a perturbed correlation peak is observed at intermediate q with a nonzero intensity at lower scattering vector. Also the covalent comb is slightly affected in this q-range.

The scattering profile of the functionalized system is the result of the equilibrium between a diblock copolymer arising from the association of thy- and DAT-functionalized chains in a comblike arrangement and single nonattached short chains. The scattering study, therefore confirms a dominant heterocomplementary mechanism involving the association of the two different complementary groups (thy-DAT) and leading to the formation of a reversible comblike structure. By means of the RPA model developed for the specific

TABLE II. Sample classification.

Reversible combs	Molar ratio	Backbone volume fraction (ϕ_b)
d-PBO 80k-thy:PBO 15k-DAT	1:1	~0.25
PBO 40k-thy:PBO 15k-DAT	1:1	~0.25
Nonassociating blend	Molar ratio	ϕ_b
d-PBO 80k:PBO 15k	1:1	~0.25

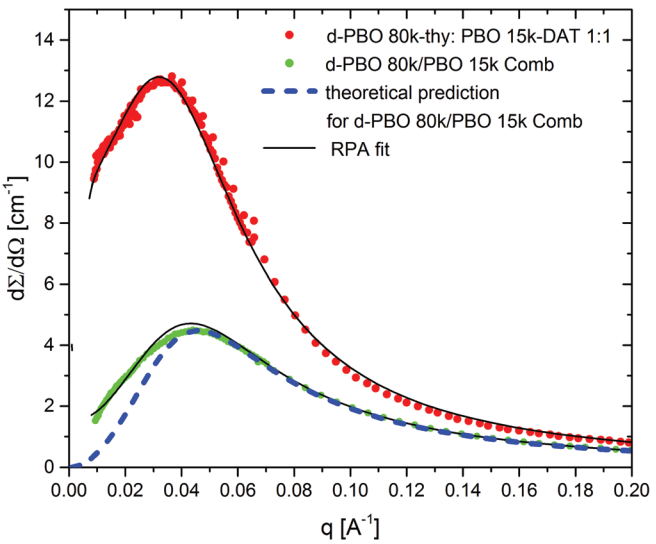

FIG. 2. Equimolar functionalized blend of H- and D-components (red) and permanent comb d-PBO 80k/PBO 15k Comb (green) at $T = 5\,^{\circ}\mathrm{C}$ with corresponding RPA fit (black lines). The stoichiometry of the samples was constant within the best-possible agreement and small intensity differences are due to statistical deviations in concentration and different absolute calibration of the intensities of the different samples.

case of this reversible comb block copolymer it was possible to determine the average aggregation number, and therefore, to estimate the effective association constant in the melt state. We found an average arm number of ~7 for an equimolar 1:1 blend in spite of 15 possible aggregation sites from the chemical analysis. This is probably due to some inaccessibility of the bonding groups. The random placement of the thy-groups—by the copolymerization of BO with a vinyl-containing monomer [20]—may lead to some too closely spaced docking places that do not allow or disfavor neighboring associations to take place. In view of the further investigation, we note that the equilibrium between the comb and free chains may possibly also slightly affect the viscoelastic and dielectric behavior since the arms should relax much faster and would not disturb the interesting intermediate-to-long-time behavior. For the estimation of the association constant K_a the average aggregation number found from SANS was used. Following the van't Hoff equation as usual the activation energy related to hydrogen bonds in the associating system can be determined from the dependence of K_a on the temperature

$$\ln K_a = \frac{-\Delta H}{RT} + \frac{\Delta S}{R}.$$

For triple hydrogen bonds in solution, the typical interaction energy was estimated in the order of 13–20 kJ/mol[10]. In the present system under investigation in the bulk, however, a value of activation energy $\Delta H \sim 6.5$ kJ/mol was obtained. As explained before, the association constant is influenced by the accessibility of the thy-groups attached to the backbone. We anticipate here that in the temperature range analyzed by SANS, the dynamics of the present polymer systems is dominated by the flow regime. In order to study the whole relaxation spectrum, rheology experiments must be conducted at lower temperature, and therefore, different aggregation numbers may appear in the dynamic-mechanical study. The extrapolation of K_a to the reference temperature of the rheology spectra ($T = -25°C$) yields an average aggregation number for the transient comb of ~12 arms. The latter value is close to the maximum number of available aggregation sites, although the association might still be limited somewhat by possible sterical hindrance effects.

The permanent comb d-PBO 80k/PBO 15k Comb shows a different scattering function from the functionalized blend. The lower amplitude of the peak intensity agrees with the larger number of arms in comparison to the reference functionalized mixture. However, an additional finite scattering intensity, not predicted in the theoretical scattering function of a full 15 arms comb, is observed in the experimental data at low q, in spite of the extreme purity of the sample revealed by chemical characterization. For this reason, the description with the same RPA model is required to take into account a fraction on nonattached species. An average number of ~12 arms was then estimated, in fair agreement with 15 expected. Note that this value is very close to the average aggregation number for the analog transient comb extrapolated to $T = -25°C$. We remind that the permanent comb was synthesized from the same parent PBO and therewith a similar distribution of groups is expected. However, the synthesis is of the type grafted-form which favors all sites to be activated by the initiator and growth of the chains to occur independently. The RPA model fitted the intermediate q range sufficiently well but a good description of the low q region is not accomplished. A more accurate description should include a modeling of the possible side products present in the comb material, in the same way as was proposed in the past for partially labeled H-shaped [33] polymers which, according to GPC, were perfect and monodisperse but SANS discovered a strongly heterogeneous mixture in arm functionality, and inherent to this, also the isotopic composition. For this purpose, an adequate description of the system as a linear combination of differently functional combs would require a full knowledge of the molecular weight and arm distribution which is not available through any method.

To finalize the structural study, we showed that the nonbonding mixture corresponded to a random blend of both chains and is described by the above RPA model without interchain correlation. We note that roughly the same Flory–Huggins parameters were obtained in all three samples. We refer to our former work [19].

B. Linear rheology

Experimental mastercurves obtained for both permanent PBO combs are reported in Fig. 3 at the reference temperature $T = -25°C$ with the corresponding fit curves using the Inkson model. The Fourier transformation of the relaxation modulus $G(t)$ defined in Eq. (7) into the ω-domain to obtain $G'(\omega)$ and $G''(\omega)$ was performed numerically using a Gaussian adaptive integration routine. The data description was performed with τ_e, G_N^0, and f (see Sec. III) as refining parameters, while the dilution factor α was fixed to 1. The fitted parameters for the two permanent combs studied are reported in Table III. The important characteristic parameters for linear PBO were estimated by means of a Likhtman–McLeish fit [34] to entangled PBO 40k. For this system the entanglement molecular weight was fitted to be $M_e = (7980 \pm 350)$g/mol and the reptation time, corrected for contour length fluctuations (CLF) was found to be $\tau_{df} = (0.45 \pm 0.05)$s at $T = -25\,°C$.

The PBO 40k/PBO 15k Comb [Fig. 3(a)] shows a small plateau at intermediate frequency with a slight decrease of the elastic modulus in the arm retraction domain. At times longer than the inverse crossover frequency between G' and G'' occurring at ~10 rad/s the modulus decreases due to dilution of the backbone tube diameter with the retracted arm material. These relaxation processes are emphasized in the representation of $\tan\delta$. However, due to the low separation between the retraction time of the 15k arms and the estimated reptation time of the PBO 40k backbone the two characteristic processes are not well distinguishable as predicted, and thus, the claimed hierarchical relaxation processes that are characteristic for the present comb polymer cannot be clearly detected in the viscoelastic curve. This hierarchical relaxation is instead more evident in the case of the d-PBO 80k/PBO 15k Comb [Fig. 3(b)]. A close-to-Rouse-like mode ($\omega^{1/2}$) is experimentally found at long times, typical of a

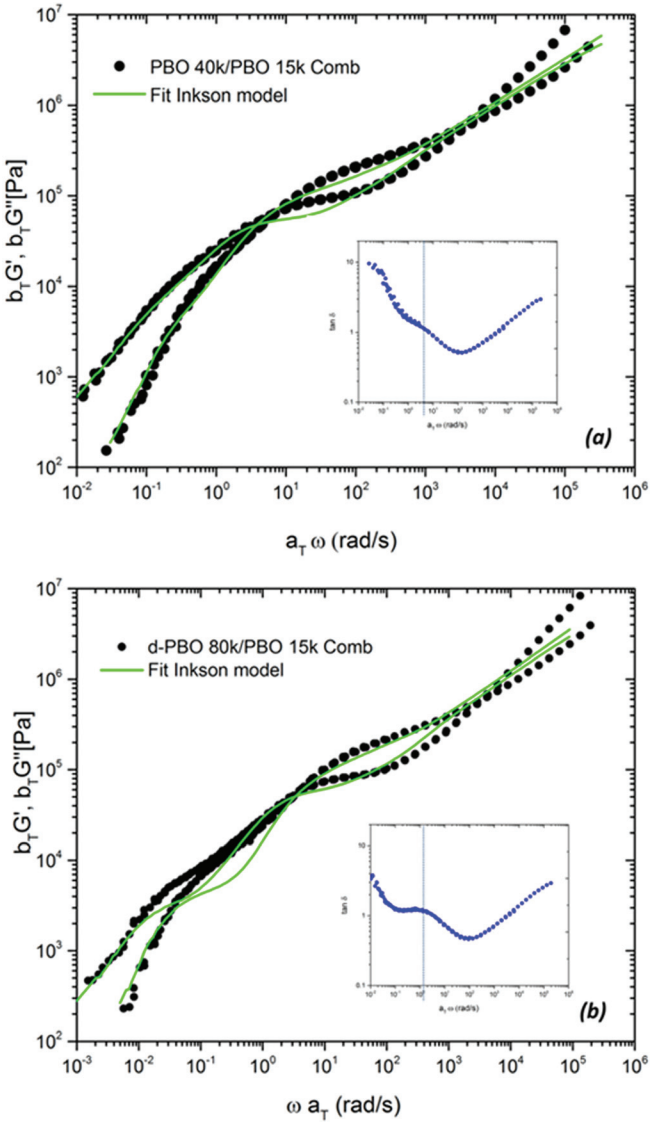

FIG. 3. Storage and loss moduli for PBO 40k/PBO 15k Comb (a) and d-PBO 80k/PBO 15k Comb (b) at $T_{\mathrm{Ref}} = -25\,^{\circ}\mathrm{C}$. Fit with Inkson model (green lines).The insets show the loss factor tan δ.

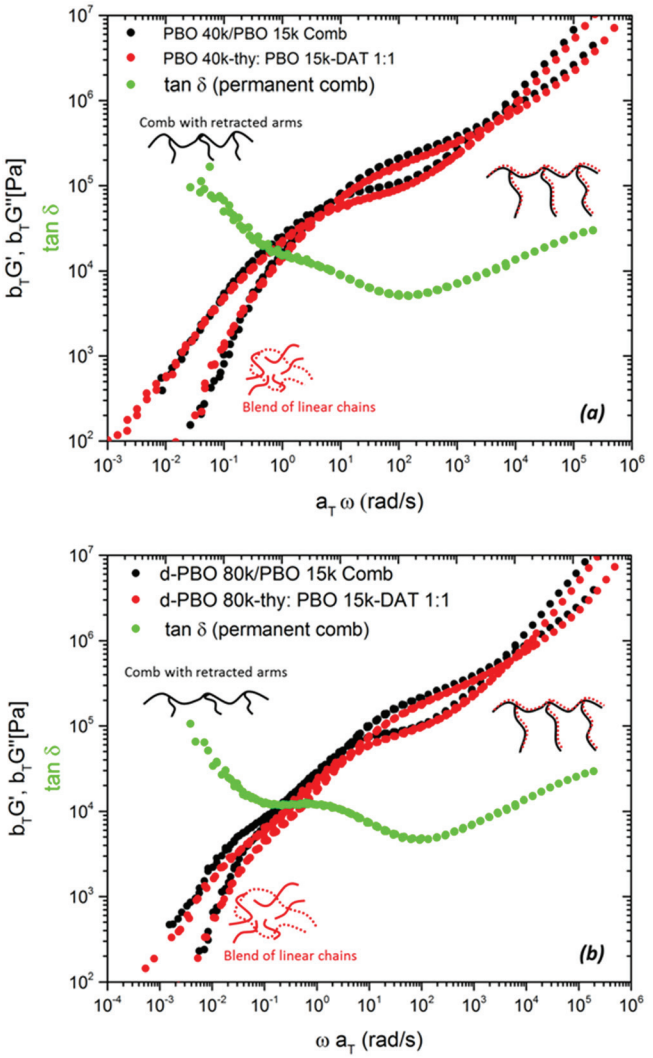

FIG. 4. Comparison of G' and G'' of permanent (black) and supramolecular combs (red) with identical composition at $T_{\mathrm{Ref}} = -25\,^{\circ}\mathrm{C}$. tan δ (green) is given for the permanent combs. The sketches tentatively indicate the splits of the dynamic spectrum into comb architecture and bimodal blends.

nonentangled chain but which now corresponds to the reptation of the backbone in a dilated tube of which the diameter is the end-to-end distance of the backbone polymer. The different low frequency behavior in both combs is ascribed to the different volume fractions of the short chains which are either too small or just large enough to cause the complete dilution of the backbone tube. Although the best fits with the upper model that are shown in Fig. 3 sufficiently match the experimental data, major discrepancies are noticeable in the cross-over region between the two hierarchical levels due to remaining inadequacies of the model, like the neglect of polydispersity and some model-internal assumptions. The estimated values (Table III) for τ_e and G_N^0 are in good agreement with the literature results [20,35] obtained for PBO linear chains. The number of arms estimated from the fit in both cases deviate from the values provided by the GPC analyses. The distance between the graft arms, however, is on average constant and about 1 entanglement mesh long (∼8000 g/mol).

In the case of the smaller PBO 40k/PBO 15k Comb the determination of the average arm number is limited by the sensitivity of the models shown in Fig. 1. For d-PBO 80k/PBO 15k Comb the estimation of f is instead more accurate. The smaller discrepancy between the estimated value and the one provided by chemical characterization is due to the timely more pronounced separation of both characteristic processes of relaxation. We note that the number of arms found using the Inkson approach is in good agreement with the SANS data and indirectly confirms that other comb-shaped polymers that show this dynamic fingerprint in the

TABLE III. Fit parameters for permanent combs.

PBO 40k/PBO 15k Comb	
G_N^0 (Pa)	$(2.6\pm0.1)\times10^5$
f	(3.8 ± 0.3)
τ_e(s)	$(2.3\pm0.2)\times10^{-3}$
d-PBO 80k/PBO 15k Comb	
G_N^0 (Pa)	$(2.6\pm0.08)\times10^5$
f	(11 ± 0.4)

samples are present, and therefore, were not detected in the molar mass distribution by GPC. The strong dependence of the SANS peak height on f is an asset of the scattering study in these systems.

In Figs. 4(a) and 4(b) the dynamic moduli of the permanent combs are compared with the ones for the analogs reversible combs, this time resulting from 1:1 combinations of thy- and DAT-functionalized linear chains. The systems have therewith identical compositions, i.e., identical volume fraction of arms and backbone and the corresponding mastercurves are reported at the reference temperature $T_0 = -25°C$. Permanent and reversible combs exhibit a very similar viscoelastic behavior. The permanent comb model of Inkson would thus describe the reversible comb equally as well in the whole frequency range. We refer to our former work [19,20] where nonfunctionalized mixtures were shown to be faster by orders of magnitude.

For the permanent combs, the two maxima in G'' are attributed to the retraction of the arms and the reptation of the diluted backbone. The relaxation process of a supramolecular comb is instead determined by the lifetime of the transient bonds between arms and backbone. For time scales shorter than the hydrogen bond lifetime, a permanent comblike behavior with a characteristic hierarchical relaxation scheme would be expected. On the other hand, when the reversible bonds are not effective anymore, the system would act as a simple bimodal blend of linear chains. In our previous investigation of transient combs [19] with different arm lengths, an estimation of the lifetime from a Maxwell-like element could be obtained. A peak at intermediate frequencies in G'' was reported for the transient combs with different arm lengths and seemed to be rather independent on the size of the arms as well as on the composition of the mixtures, although the dilution behavior was changed considerably. This process was therefore attributed to the association/breakage of the transient bonds and could be approximated by such an independent additional Maxwell element with characteristic time $\tau_b \sim 1\,\mathrm{s}$. From $\tan\delta$ (green curve) the comparison with the real combs with identical composition evidences, however, a similarity between the lifetime of the thy-DAT bonds and the retraction time of the arms τ_a. Therefore, this leads to a very similar viscoelastic behavior in the two systems. At times shorter than τ_b the functionalized mixtures show a slightly lower plateau modulus in comparison with the analog permanent combs, probably due to the predilution effect exerted by the free unassociated chains, which are in steady equilibrium with the comb structure. The size of this is low as at $T = -25\,°C$ most bonds would be in the closed state. At longer times the dynamics of the functionalized mixtures is dominated by the backbone, diluted by nonconnected arms, whereas for the permanent comb, the retracted arms act as friction points for the diluted backbone, as illustrated in Fig. 4. The longer time behavior of covalent and transient combs is not distinguishable due to the same dilution effect exerted by retracted and nonconnected arms, except for a higher friction provided by the branching point in the case of the covalent comb.

The similar viscoelastic response observed for permanent and reversible combs indicates that a coincidence of the two different intermediate processes, referring, respectively, to the lifetime of the transient bonds and the retraction time of the 15k branches would lead to a comblike behavior in the whole frequency range.

C. Dielectric spectroscopy

Broadband dielectric spectroscopy (BDS) is known to be a valuable additional tool as well to investigate dynamic processes in polymers through measurements of the dipolar relaxation in an oscillating electric field. Whereas in linear polymers the end-to-end vector relaxation can be followed isothermally over a broad range of frequencies, for structurally branched systems, the end-to-branch-point vectors must be considered and also the topology of the branching cannot be disregarded. In our study, the imaginary component of the dielectric permittivity (ε'') is shown at the same reference temperature $T = -25°C$ as the linear rheology but in a single frequency scan over almost 8 decades. This avoids any application of a time-temperature superposition for activated processes as is needed in the corresponding mechanical-rheological spectroscopy. The BDS experiments, presented in Fig. 5(a) were carried out on a permanent PBO comb polymer, the corresponding mixture of thy- and DAT-functionalized chains as well as on a nonassociating mixture. Furthermore, the single backbone in both functionalization states was studied. In Fig. 5(a) the loss part of the dielectric permittivity ε'' is reported on the common frequency scale f in Hz. Note that for clarity the dielectric functions were arbitrarily shifted along the y-axis so that a better distinction of the relaxation processes involved in the different curves is allowed. Within experimental error, the α peak of all samples was almost of identical amplitude, showing that the thickness of the samples was very comparable. The curves in Fig. 5(a) were scaled in three sets: The lower backbones (shifted down by a factor of $\sim$10), the upper comb samples (shifted up by a factor of $\sim$2), and in the middle a simple blend of which the position on the y-axis is kept constant as reference. The shifts were varied for illustrative purposes.

We emphasize further that the presented data correspond already to the same state in view of the constant DSC glass transition temperature measurements, and thus, no horizontal adjustment of the frequency axes was needed. Since no direct comparison of the BDS data with a molecular rheo-dielectric model for comblike architectures is available in the literature, the following discussion will be entirely based on the relation between the spectra.

In agreement with the DSC results, the local or segmental relaxation time τ_α is identical for all presented samples. Therefore, the monomeric friction coefficients are very similar as well.

In order to investigate the effect of the thy groups on the dielectric response of reversible combs in Fig. 5(a), as a reference, we show ε'' of the pure thy-modified and nonfunctionalized backbone. From the figure, the pure backbone polymer exhibits the typical behavior of a long entangled linear chain. Its frequency dependence in the intermediate time range is $f^{-1/4}$ as the result of CLF mechanism [36,37]. The break in the $-1/4$ slope into a higher dependence observed at

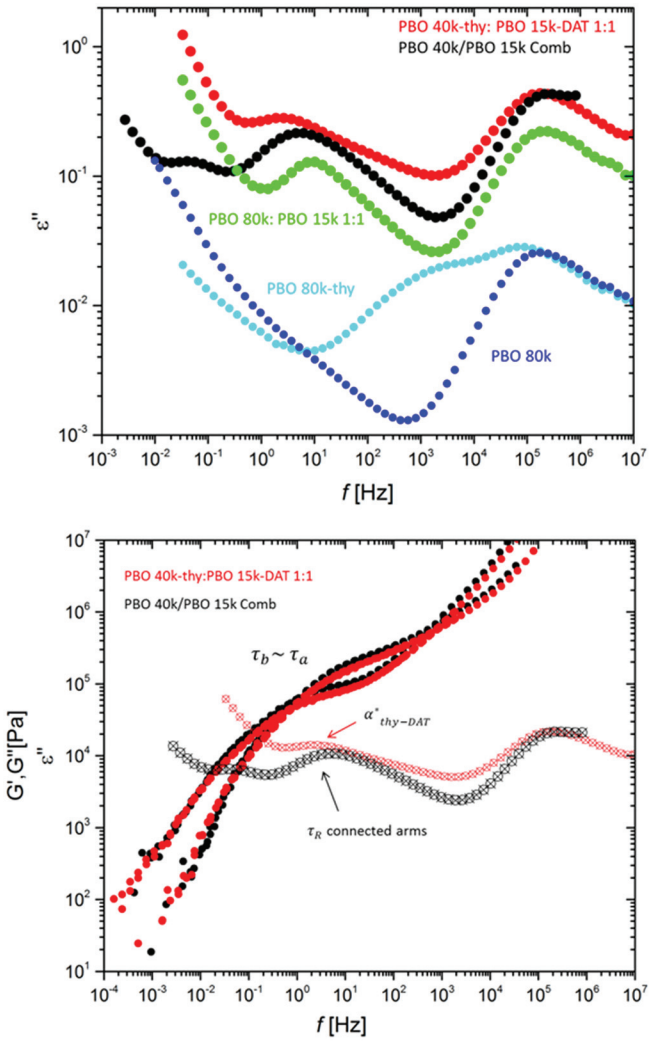

FIG. 5. (a) Dielectric response for PBO 40k-thy:PBO 15k-DAT 1:1 (red), PBO 40k/PBO 15k Comb (black) and d-PBO 80k:PBO 15k 1:1 (green). Pure backbones d-PBO 80k (blue) and d-PBO 80k-thy (cyan) are shown as references on the bottom at $T = -25\,^{\circ}\mathrm{C}$. The red and black curves were shifted up by a factor of 2 along the y-axis. The cyan and blue curves were shifted down by a factor of 10 along the y-axis while the green curve was not shifted and kept as reference. (b) Comparison between viscoelastic and dielectric response for permanent (black) and transient (red) combs.

low frequency is due to the transition to slower reptation dynamics ($\sim f^{-1/2}$) and the time scale is in very good agreement with the estimate from the Rouse time of the backbone polymer,

$$\tau_R = \tau_e Z^2,$$

where $Z \sim 10$ is the number of entanglement for PBO 80k. Whereas these rheological fingerprints are scarce but some examples are available since other many processes like CR or even polydispersity obstruct their visibility, BDS, on the other hand, is very sensitive. Experimental verification and the almost ideal presence can be found in [34,36,37]. Further interpretations are, however, hampered by the ionic conductivity contributing with f^{-1}. The global relaxation of the thy-modified 80k PBO backbone (d-PBO 80k-thy), on the other hand, is strongly affected by the random introduction of the supramolecular groups along the backbone contour. The additional peak showing up in the supramolecular backbone spectrum around 10^3 Hz is assigned to the momentarily well-debated α^* process [38,39]. The latter arises if the opening of a transient bond gives rise to a dipole moment change as was recently discussed on a structurally similar bifunctional urazole linker distributed on long polyisoprene chains [40]. In the present thy-thy dis- and reassociation of entangled PBO backbones this process seems to occur on a time scale $\tau^*_\alpha \sim 1.5\ 10^{-4}$ s, which is much shorter than the entanglement time, and therefore, will have no influence on the chain entanglement dynamics in rheology as reported in the literature [20]. This self-complementary association, however, is strong in the BDS response, due to the high dipole moment of the polar thy group itself. The closed state of thy-thy bonds effectively erases the dipole moment.

We now address the mixtures of different components. The nonfunctionalized mixture of pure 15k arms and pure backbone d-PBO 80k:PBO 15k 1:1 (green curve) shows at least 2 peaks in the dielectric response. The single narrow-distributed peak observed at lower frequency is assigned to the Rouse-time of the short component while the terminal relaxation of the long chain is hidden by the parasitic conductivity contribution. The characteristic time of the short chain is about 0.015 s, slightly larger than the pure Rouse time (0.01 s) due to the tube environment of the long chains.

This bimodal blend is now taken as the reference for the two branched architectures. Since the normal mode of the 80k-backbone at low f could obviously not be detected, we present the permanent comb sample that is based on the shorter 40k backbone but with the same 15k graft arms. In this particular case, the ε'' data obtained at $-5^{\circ}\mathrm{C}$ are included in order to capture the normal mode of the backbone more clearly. These data were properly shifted to the reference temperature of $-25\,^{\circ}\mathrm{C}$. First, the permanent comb (black curve) is discussed: Three peaks can be discerned. The intermediate peak width related to the arms is narrow and a closer inspection reveals that the peak frequency is shifted by a factor ~3–4 to lower frequencies, compared to the random mixture before. This shift toward longer times can be theoretically shown to correspond to the Rouse time of a chain, which is fixed at one end [41]. The distribution remains unaltered and this serves as an experimental proof for the small arm length polydispersity index. As a further experimental proof, the third peak on the left which is shallow but clearly visible at ~0.05 Hz with $\tau \sim 3$ s compares fairly well to the terminal time of reptation of the backbone, $\tau_d \sim 1$ s, without CLF. Whereas CLF is active in the pure backbone, here, it is suppressed due to the presence of the new friction blobs that the retracted arms make. The latter, however, perform a related CLF, i.e., retraction toward the branching point, which follows a similar $f^{-1/4}$ dependence as seen in the high-frequency wing of the arm peak in BDS.

Second, the transient comb can be discussed in comparison to its permanent analog. Figure 5(a) shows that the intermediate f_{peak} for the associating mixture PBO 40k-thy:PBO 15k-DAT 1:1 (red curve) occurs at about the same time or even at slightly longer time than for the analog comb. In Fig. 5(b) the rheological and dielectric results obtained for permanent and reversible combs are reported on the common

Hz scale. The viscoelastic relaxation processes attributed to τ_a and τ_b, respectively, for permanent and transient combs are related to the intermediate frequency peaks in ε'' occurring in the same frequency range. However, although the lifetime of the bonds and the retraction time of the fixed arms cannot be distinguished in the dynamic moduli, the dielectric response is clearly more sensitive in the identification of the different relaxation processes. The characteristic low frequency peak in the functionalized mixture, attributed to the $\alpha^*_{\text{thy–DAT}}$ process, occurs at slightly longer times than the Rouse mode of the fixed arms leading to the observation of a comblike behavior in the whole frequency range, as tentatively represented by the arrows in the figure. The broader spectrum must be due to additional contributions. Dissociation has led to a strong contribution in the case of thy groups, which can be considered to be incoherently added to the polymer-related dielectric response. Broadening toward lower f, i.e., longer time is instead assigned to the normal mode of the arms, after the thy-DAT disconnection in an $\alpha^*_{\text{thy–DAT}}$ process has taken place. We emphasize that the complementary dielectric investigation allowed a more accurate distinction of the processes identified in the viscoelastic spectra.

V. CONCLUSION

With the combination of the different techniques for the study of branching interactions in supramolecular-active polymers, details about the heterocomplementary hydrogen bonding in thy-DAT complexes and their consequences could be revealed. The present study completes a former work [19,20] in that a dynamic mixture is compared in a 1-to-1 fashion to the permanent covalent branched architecture. We summarize the achievements as follows: (i) SANS was used to confirm the envisaged comblike architecture, which should install itself by the directed association of thy- and DAT functions on different components, which additionally could be distinguished by a different H/D isotopic labeling. The RPA correlation peak and deviation from it served to derive the equilibrium constant or equivalently the average functionality of the comb as $f(T)$. (ii) the rheology of the dynamic mixture and permanent combs depends on the stoichiometry of the blend and is at maximum identical or always between the permanent and unlinked mixture. A molecular-rheological approach for permanent combs could be shown to be in fair agreement. First indications about the origin of the intermediate dissipation peak, i.e., either retraction of the arms or a finite lifetime of the thy-DAT bonds or simultaneous appearance became clear as its characteristic frequency hardly depended on the length of the involved arms. (iii) The dielectric response also confirmed the architecture but at the same time showed short-lived parallel homoassociations (thy-thy) of the backbones to appear. (iv) Furthermore as a general conclusion the lifetime of the thy-DAT bonding was found to be $\sim$2 times longer than the retraction time of the barely entangled arms. Work is in progress to extend the study to shorter and longer grafting arms, connected to the same backbone length by which the hierarchical relaxation in the comb becomes timely separated around the present estimate of $\sim$1–2 s at $T = -25\,^{\circ}\text{C}$. This time scale, converted to ambient temperatures, assumes exploitable values (20–50 Hz) for common processes in industrial extrusion or mixing, for dampening effects of mechanical vibrations in e.g., transport or self-healing in commodity goods.

ACKNOWLEDGMENTS

The authors thank the financial support of the EU (ITN SASSYPOL 607602 Marie Curie Network). The authors acknowledge Dr. Nicole Lühmann for the help in the NMR analysis.

References

[1] Brunsveld, L., B. J. B. Folmer, E. W. Meijer, and R. P. Sijbesma, "Supramolecular polymers," Chem. Rev. **101**, 4071–4098 (2001).

[2] de Greef, T. F. A., and E. W. Meijer, "Material science: Supramolecular polymers," Nature **453**, 171–173 (2008).

[3] Aida, T. A., E. W. Meijer, and S. I. Stupp, "Functional supramolecular polymers," Science **335**, 813–817 (2012).

[4] Nair, K. P., J. M. Pollino, and M. Weck, "Noncovalently functionalized block copolymers possessing both hydrogen bonding and metal coordination centers," Macromolecules **39**, 931–940 (2006).

[5] Stadler, F. J., W. Pyckhout-Hintzen, J. M. Schumers, C. A. Fustin, J. F. Gohy, and C. Bailly, "Viscoelastic rheology of moderately entangled telechelic polybutadiene temporary networks," Macromolecules **42**, 6181–6192 (2009).

[6] Scott Lokey, R., and B. L. Iverson, "Synthetic molecules that fold into a pleated secondary structure in solution," Nature **375**, 303–305 (1995).

[7] Binder, W. H., and Zirbs, R., "Supramolecular polymers and networks with hydrogen bonds in the main and side-chain," Adv. Polym. Sci. **207**, 1–78 (2007).

[8] Anthamatten, M., "Hydrogen bonding in supramolecular polymer networks: Glasses, melts, and elastomers. Supramolecular polymer networks and gels," Adv. Polym. Sci. **268**, 47–98 (2015).

[9] Brás, A. R., C. H. Hövelmann, W. Antonius, J. Teixeira, A. Radulescu, J. Allgaier, W. Pyckhout-Hintzen, A. Wischnewski, and D. Richter, "Molecular approach to supramolecular polymer assembly by small angle neutron scattering," Macromolecules **46**, 9446–9454 (2013).

[10] Krutyeva, M., A. R. Brás, W. Antonius, C. H. Hövelmann, A. S. Poulos, J. Allgaier, A. Radulescu, P. Lindner, W. Pyckhout-Hintzen, A. Wischnewski, and D. Richter, "Association behavior, diffusion and viscosity of end-functionalized supramolecular poly(ethylene glycol) in the melt state," Macromolecules **48**, 8933–8946 (2015).

[11] Lou, N., Y. Wang, X. Li, H. Li, P. Wang, C. Wesdemiotis, A. P. Sokolov, and H. Xiong, "Dielectric relaxation and rheological behavior of supramolecular polymeric liquid," Macromolecules **46**, 3160–3166 (2013).

[12] Fox, J. D., and S. J. Rowan, "Supramolecular polymerizations and main chain supramolecular polymers," Macromolecules **42**, 6823–6835 (2009).

[13] Weck, M., "Side-chain functionalized supramolecular polymers," Polym. Int. **56**, 453–460 (2007).

[14] Yan, T., K. Schröter, F. Herbst, W. H. Binder, and T. Thurn-Albrecht, "What controls the structure and the linear and nonlinear rheological properties of dense, dynamic supramolecular polymer networks?," Macromolecules **50**, 2973–2985 (2017).

[15] Yan, T., K. Schröter, F. Herbst, W. H. Binder, and T. Thurn-Albrecht, "Nanostructure and rheology of hydrogen-bonding telechelic polymers in the melt: From micellar liquids and solids to supramolecular gels," Macromolecules **47**, 2122–2130 (2014).

[16] Courtois, J., I. Baroudi, N. Nouvel, E. Degrandi, S. Pensec, G. Ducouret, C. Chaneac, L. Bouteiller, and C. Creton, "Supramolecular soft adhesive materials," Adv. Funct. Mater. **20**, 1803–1811 (2010).

[17] Feldman, K. E., M. J. Kade, E. W. Meijer, C. J. Hawker, and E. J. Kramer, "Model transient networks from strongly hydrogen-bonded polymers," Macromolecules **42**, 9072–9081 (2009).

[18] Ahmadi, M., L. G. D. Hawke, H. Goldansazand, and E. van Ruymbeke, "Dynamics of entangled linear supramolecular chains with sticky side groups: Influence of hindered fluctuations," Macromolecules **48**, 7300–7310 (2015).

[19] Staropoli, M., A. Raba, C. H. Hövelmann, M. Krutyeva, J. Allgaier, M. S. Appavou, U. Keiderling, F. J. Stadler, W. Pyckhout-Hintzen, A. Wischnewski, and D. Richter, "Hydrogen bonding in a reversible comb polymer architecture: A microscopic and macroscopic investigation," Macromolecules **49**, 5692−5703 (2016).

[20] Allgaier, J., C. H. Hövelmann, Z. Wei, M. Staropoli, W. Pyckhout-Hintzen, N. Lühmann, and S. Willbold, "Synthesis and rheological behavior of poly(1,2-butylene oxide) based supramolecular architectures," RSC Adv. **6**, 6093–6106 (2016).

[21] See supplementary material at http://dx.doi.org/10.1122/1.5001059 for the detailed chemical characterization of the samples.

[22] Radulescu, A., N. K. Szekely, and M. S. Appavou, "KWS-2: Small angle scattering diffractometer," J. Large-Scale Res. Facil. **1**, 1–5 (2015).

[23] Watanabe, H., Y. Matsumiya, and T. Inoue, "Dielectric and viscoelastic relaxation of highly entangled star polyisoprene: Quantitative of tube dilation model," Macromolecules **35**, 2339–2357 (2002).

[24] Berry, G., S. Kahle, S. Ohno, K. Matyjaszweki, and T. Pakula,"Viscoelastic and dielectric studies on comb- and brush-shaped poly(n-butyl acrylate)," Polymer **49**, 3533–3540 (2008).

[25] Higgins, J. S., and H. Benoit, *Polymers and Neutron Scattering* (Clarendon, Oxford, UK, 1994).

[26] Hammouda, B., "Random phase approximation for compressible polymer blends," J. Non-Cryst. Solids **172–174**, 927–931 (1994).

[27] Read, D. J., "Mean field theory for phase separation during polycondensation reactions and calculation of structure factors for copolymers of arbitrary architecture," Macromolecules **31**, 899–911 (1998).

[28] Benoit, H., and G. Hadziiannou, "Scattering theory and properties of block copolymers with various architectures in the homogeneous bulk state," Macromolecules **21**, 1449–1464 (1988).

[29] Inkson, N. J., R. S. Graham, T. C. B. McLeish, D. J. Groves, and C. M. Fernyhough, "Viscoelasticity of monodisperse comb polymer melts," Macromolecules **39**, 4217–4227 (2006).

[30] Kapnistos, M., D. Vlassopoulos, J. Roovers, and L. G. Leal, "Linear rheology of architecturally complex macromolecules: Comb polymers with linear backbones," Macromolecules **38**, 7852–7862 (2005).

[31] McLeish, T. C. B., and S. T. Milner, "Entangled dynamics and melt flow of branched polymers," Adv. Polym. Sci. **143**, 195–256 (1999).

[32] McLeish, T. C. B., J. Allgaier, D. K. Bick, G. Bishko, P. Biswas, R. Blackwell, B. Blottière, N. Clarke, B. Gibbs, D. J. Groves, A. Hakiki, R. K. Heenan, J. M. Johnson, R. Kant, D. J. Read, and R. N. Young, "Dynamics of entangled H-polymers: Theory, rheology, and neutron-scattering," Macromolecules **32**, 6734–6758 (1999).

[33] Perny, S., J. Allgaier, D. Cho, W. Lee, and T. Chang, "Synthesis and structural analysis of an H-shaped polybutadiene," Macromolecules **34**, 5408–5415 (2001).

[34] Likhtman, A. E., and T. C. B. McLeish, "Quantitative theory for linear dynamics of linear entangled polymers," Macromolecules **35**, 6332–6343 (2002).

[35] Gerstl, C., G. J. Schneider, W. Pyckhout-Hintzen, J. Allgaier, D. Richter, A. Alegria, and J. Colmenero, "Segmental and normal mode relaxation of poly(alkylene oxide)s studied by dielectric spectroscopy and rheology," Macromolecules **43**, 4968–4977 (2010).

[36] Glomann, T., G. J. Schneider, A. R. Brás, W. Pyckhout-Hintzen, A. Wischnewski, R. Zorn, J. Allgaier, and D. Richter, "Unified description of the viscoelastic and dielectric global chain motion in terms of the tube theory," Macromolecules **44**, 7430–7437 (2011).

[37] Unidad, H. J., M. Abdel Goad, A. R. Brás, M. Zamponi, R. Faust, J. Allgaier, W. Pyckhout-Hintzen, A. Wischnewski, D. Richter, and L. J. Fetters, "Consequences of increasing packing length on the dynamics of polymer melts," Macromolecules **48**, 6638–6645 (2015).

[38] Müller, M., U. Seidel, and R. Stadler, "Influence of hydrogen bonding on the viscoelastic properties of thermoreversible networks: Analysis of the local complex dynamics," Polymer **16**, 3143–3150 (1995).

[39] Shabbir, A., H. Goldansaz, O. Hassager, E. van Ruymbeke, and N. J. Alvarez, "Effect of hydrogen bonding on linear and nonlinear rheology of entangled polymer melts," Macromolecules **48**, 5988–5996 (2015).

[40] Gold, B. J., C. H. Hövelmann, N. Lühmann, N. K. Székely, W. Pyckhout-Hintzen, A. Wischnewski, and D. Richter, "Importance of compact random walks for the rheology of transient networks," ACS Macro Lett. **6**, 73–77 (2017).

[41] Willner, L., R. Lund, M. Monkenbusch, O. Holderer, J. Colmenero, and D. Richter, "Polymer dynamics under soft confinement in a self-assembled system," Soft Matter **6**, 1559–1570 (2010).